



HAL
open science

Time-lapse and cell ablation reveal the role of cell interactions in fly glia migration and proliferation

Benoît Aigouy, Véronique van de Bor, Marcel Boeglin, Angela Giangrande

► To cite this version:

Benoît Aigouy, Véronique van de Bor, Marcel Boeglin, Angela Giangrande. Time-lapse and cell ablation reveal the role of cell interactions in fly glia migration and proliferation. *Development* (Cambridge, England), 2004, 131 (20), pp.5127-5138. 10.1242/dev.01398 . hal-03447948

HAL Id: hal-03447948

<https://hal.science/hal-03447948>

Submitted on 15 Dec 2021

HAL is a multi-disciplinary open access archive for the deposit and dissemination of scientific research documents, whether they are published or not. The documents may come from teaching and research institutions in France or abroad, or from public or private research centers.

L'archive ouverte pluridisciplinaire **HAL**, est destinée au dépôt et à la diffusion de documents scientifiques de niveau recherche, publiés ou non, émanant des établissements d'enseignement et de recherche français ou étrangers, des laboratoires publics ou privés.

Time-lapse and cell ablation reveal the role of cell interactions in fly glia migration and proliferation

Benoît Aigouy, Véronique Van de Bor*, Marcel Boeglin and Angela Giangrande†

Institut de Génétique et Biologie Moléculaire et Cellulaire, IGBMC/CNRS/ULP/INSERM – BP 10142, ILLKIRCH, C. U. de Strasbourg, 67404, France

*Present address: University of Edinburgh, Wellcome Trust Centre for Cell Biology, King's Buildings, Mayfield Road, Edinburgh, EH9 3JR, UK

†Author for correspondence (e-mail: angela@titus.u-strasbg.fr)

Accepted 12 August 2004

Development 131, 5127–5138
Published by The Company of Biologists 2004
doi:10.1242/dev.01398

Summary

Migration and proliferation have been mostly explored in culture systems or fixed preparations. We present a simple genetic model, the chains of glia moving along fly wing nerves, to follow such dynamic processes by time-lapse in the whole animal. We show that glia undergo extensive cytoskeleton and mitotic apparatus rearrangements during division and migration. Single cell labelling identifies different glia: pioneers with high filopodial, exploratory, activity and, less active followers. In combination with

time-lapse, altering this cellular environment by genetic means or cell ablation has allowed us to define the role of specific cell-cell interactions. First, neurone-glia interactions are not necessary for glia motility but do affect the direction of migration. Second, repulsive interactions between glia control the extent of movement. Finally, autonomous cues control proliferation.

Key words: Glia, Migration, Proliferation, Drosophila, Time-lapse

Introduction

In order to migrate properly, cells respond to environmental cues that control the extent and direction of migration. In many cases, migration is associated with proliferation, the orchestration of the two processes being crucial for final tissue/organ architecture.

Migration and proliferation have been extensively characterised in fixed tissues or by time-lapse in cell cultures (e.g. Etienne-Manneville and Hall, 2003; Friedl and Wolf, 2003; Fulga and Rorth, 2002; Gerlich et al., 2003; Lauffenburger and Horwitz, 1996; Meili and Firtel, 2003; Welch et al., 1997). Ideally, however, one would like to analyse such dynamic events by time-lapse in the whole animal and to follow individual cells. The advent of green fluorescent protein (GFP) as a marker of living cells has opened new perspectives in the field (e.g. Bellaïche et al., 2001; Gilmour et al., 2002; Kakita, 2001; Kaltschmidt et al., 2000; Nadarajah and Parnavelas, 2002; Ribeiro et al., 2002; Wood et al., 2002).

In the peripheral nervous system (PNS), glia represent a typical example of migratory cells. The fact that PNS glia follow axons [fly wing glia (Giangrande, 1994), fly embryo (Sepp et al., 2000), zebrafish lateral line (Gilmour et al., 2002), chicken Schwann cells (Carpenter and Hollyday, 1992)] and migrate as chains of cells strongly suggests that cell-cell interactions play a role in migration and/or proliferation. The bilayered organisation of the fly wing epithelium and the presence of purely sensory nerves constitute advantageous features to study cell migration and proliferation in vivo. Moreover, the origin of wing glial cells has been characterised (Giangrande et al., 1993; Giangrande, 1994; Van De Bor et al., 2000). We have therefore established a confocal non-invasive

approach that makes it possible to follow wing glial cells by time-lapse in the whole animal.

We show that extensive and dynamic cell shape remodelling allows glia to polarise along the underlying axon during migration and proliferation. We also identify two populations of migratory cells, pioneer glia, which explore the environment by extending long filopodia, and follower glia, which are less active. Furthermore, we have determined a confocal-assisted ablation protocol that can be used for single cells, which represents a novel and useful tool over the conventional bright-field optic setups. The combined use of time-lapse, cell ablation and genetic manipulation has enabled us to identify the contribution of different cell-cell interactions to distinct aspects of glial cell development: (1) glia-glia interactions control the extent of glia migration; (2) neurone-glia interactions are not necessary for glia motility but do affect the direction of glia migration; and (3) autonomous cues control the final number of glial cells.

Materials and methods

Fly strains and heat-shock treatments

The wild-type strain was *Sevelen*. The *repo-Gal4* driver (Sepp et al., 2001) was used to drive the following reporters: *UAS-ncGFP* (Mollereau et al., 2000) (nucleus and cytoplasm), *UAS-nlsGFP* (nucleus), *UAS-tauGFP* (Brand, 1995) (microtubule) and *UAS-actinGFP* (Verkhusha et al., 1999) (actin). *Hw^{49c/+}; UAS-ncGFP/+; repo-Gal4/+* flies and *N^{ts1}; UAS-ncGFP; repo-Gal4/Tb* flies were used for genetic analyses. *N^{ts1}* animals were kept at 18°C before and after heat shock (30°C from 6 to 12 hours APF). According to Ashburner and Thompson (Ashburner and Thompson, 1978), development at 18°C was estimated to be twice as long as at 25°C. Finally, *FRT19A/FRT19A, hs-FLP, tub-Gal80; UAS-ncGFP/+; repo-*

Gal4/+ flies were used for MARCM analysis, clones were obtained after a 37°C one-hour heat-shock at wandering L3 stage. Non-thermo-sensitive strains were raised at 25°C.

Immunohistochemistry

Fixation, dissection and antibody incubation were performed as previously described (Giangrande et al., 1993), using the following antibodies: mouse anti-Repo [1:1000; Developmental Studies Hybridoma Bank (DSHB)], rabbit anti-Repo (1:4000; A. Travers), mouse anti-22c10 (Fujita et al., 1982) (1:100; DSHB), rat anti-Elav (1:500) (Robinow and White, 1991) (DSHB), rabbit anti-GFP (1:1000; Molecular Probes). TUNEL staining was performed by using the In Situ Cell Death Detection Kit (Roche) according to manufacturer's recommendations. Secondary antibodies coupled with FITC, CY3 or CY5 (Jackson) were used at 1:400. Wings were mounted in Vectashield medium (Vector Laboratories).

Time-lapse

Living pupae were taped to facilitate dissection. The puparium case was removed and the exposed wing was covered with 10S oil (Voletaf). Animals were subsequently transferred, with the wing facing down, to a glass dish (Willco-dish). Glial cells were imaged in 4D using a TCS SP2 inverted confocal microscope (Leica) equipped with a heating stage to maintain a constant temperature (25±2°C).

Confocal laser ablation

The nucleus to be targeted was selected upon GFP labelling and scanned in the z-axis to identify a focal plane located at the centre of

the nucleus in the three x, y and z axes. A region within the nucleus was chosen using the Leica bleachpoint function and submitted to UV laser irradiation (350 nm, 20 seconds pulse at medium intensity). Cell death was revealed by a strong decrease in GFP fluorescence and was confirmed by immunolabelling after fixation.

Image processing

Z-stack projections, colour coding (Bernardoni et al., 1999), rotations, figure mounting and time-lapse movies were obtained using the in-house developed TIMT software. Images were annotated using Adobe Photoshop and Illustrator, movies were converted to QuickTime format using Adobe Premiere.

Results

Glial organisation in the fly pupal wing

The fly wing contains two purely sensory nerves that navigate proximally along the so-called L1 and L3 veins (Murray et al., 1984), and are lined by glial cells (Fig. 1B,C) (Giangrande et al., 1993; Van De Bor et al., 2000; Van De Bor and Giangrande, 2002). L3 vein contains three gliogenic sensory organs, L3.3, L3.1 and L3.v (Fig. 1A,D), from distal to proximal. Each sensory organ precursor (SOP) divides asymmetrically several times and produces a glial precursor or GP, which repeatedly divides and is therefore called a first order glial precursor or GPI (Fig. 1D). The GPI, initially located adjacent to the

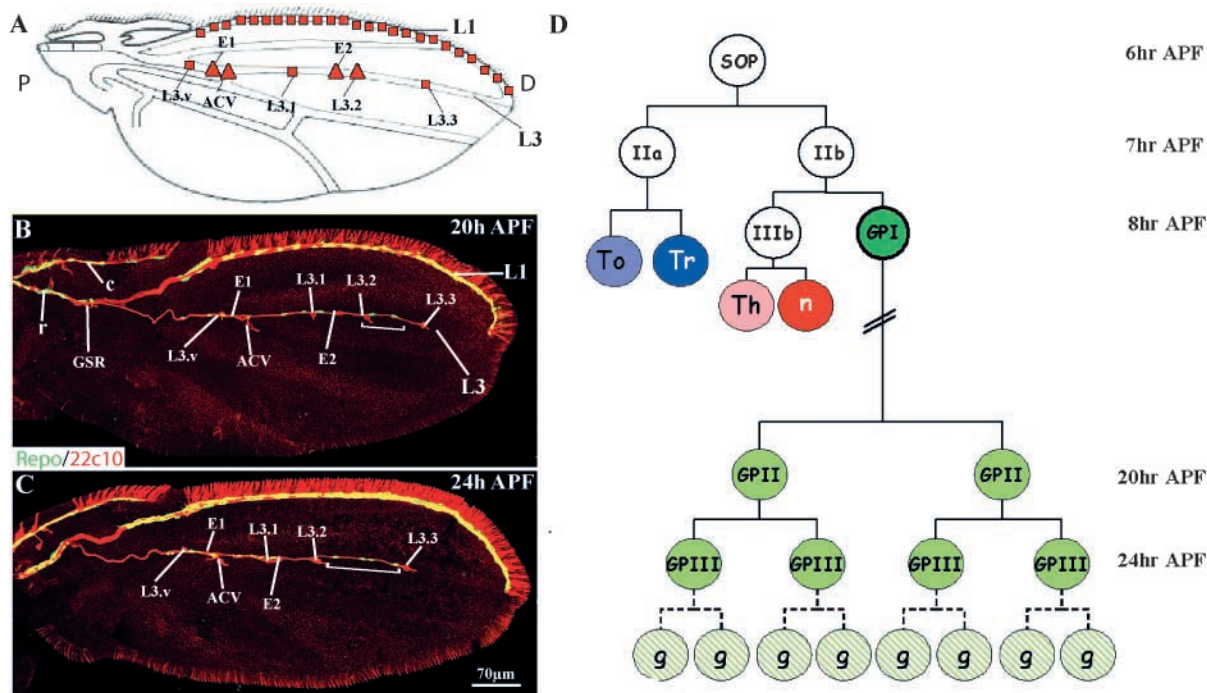


Fig. 1. Outline of glial development in the pupal wing. (A) Adult wing schematic drawing indicating the position of neurons belonging to gliogenic (squares) and non-gliogenic (triangles) sensory organs. L1 and L3 indicate L1 and L3 veins, respectively. P, proximal; D, distal. (B,C) Wild-type wings labelled with glial (anti-Repo, green) and neuronal (anti-22c10, red) markers at 20 hours after puparium formation (APF; B) and at 24 hours APF (C). GSR indicates the giant sensillum of the radius. L1, L1 nerve; L3, L3 nerve, r, radial nerve; c, costal nerve. Neurons issued from the two neurogenic (L3.2 and E2, ACV and E1) and the three gliogenic (L3.3, L3.1, L3.v) sensory organs (Van De Bor et al., 2000) are indicated. Brackets include the L3.3-derived Repo-positive cells. On this and following panels anterior is to the top, distal to the right. (D) Model for cell division in wing gliogenic sensory organs. SOP, sensory organ precursor; IIa and IIb, second order precursors; IIIb, third order precursor; To, tormogen cell; Tr, trichogen cell [also called dome/cap cell in the case of campaniform sensilla (reviewed by Keil, 1997)]; Th, thecamogen cells; n, neuron; GPI, II and III, first, second and third order glial precursors, respectively; g, glial cells. The variable number of glial cells is indicated by the dashed lines. Scale bars: 70 µm (B,C).

neuronal soma, subsequently moves along the underlying axon. The final number of glial cells per lineage varies stochastically from four to eight (average=six) (Van De Bor et al., 2000). The whole glial lineage, from GPIs to post-mitotic glial cells, expresses the Repo glial marker (Campbell et al., 1994; Halter et al., 1995; Xiong et al., 1994).

On L3, proliferation starts several hours after GPI birth, at around 17 hours after puparium formation (APF), and by 20-22 hours APF all GPIs have divided once (Fig. 1B,D) (Van De Bor et al., 2000). The second round of division takes place by 24 hours APF (Fig. 1C,D), and the third by 30 hours APF, with little glial proliferation being observed afterwards (Van De Bor et al., 2000). These data are in agreement with the GPI dividing symmetrically twice, to produce two second order and four third order precursors (GPII and GPIII, respectively, see model in Fig. 1D). The presence of up to eight glial cells suggests that GPIIIIs may or may not divide, and/or that cell death takes place throughout the lineage.

The observation that glia migrate and proliferate to variable extents (Giangrande, 1994; Van De Bor et al., 2000) suggests a role for extrinsic signals and makes it difficult to follow the development of glial lineages in fixed tissues. We therefore devised an *in vivo* glial marker by crossing the *repo-Gal4* driver (Sepp et al., 2001) with a *UAS-GFP* reporter (*repo-GFP*).

4D gliogenesis: migration and cytoskeleton remodelling

For time-lapse analyses on *repo-GFP* pupae, we removed the puparium case over the wing, leaving the appendage in place (Fig. 2A). Due to high levels of autofluorescence, wings were analysed by confocal microscopy (Z stacks of 20-100 optical sections taken at intervals ranging from 90 seconds to 15 minutes). *In vivo* GFP labelling is comparable to that observed after immunohistochemistry of fixed preparations (data not shown). Moreover, processing and laser excitation do not have a major impact on development, as pupae that have been

Table 1. L1 glia proliferation

Hours APF	L1 (n=21)	
	Repo+ cells	Repo+ and PH3+ cells
20	53-65 (60)	1-3 (1.15)
22	55-74 (68)	0-7 (2.85)
24	66-85 (75.7)	0-2 (1.4)

Twenty-one pupal wings were scored for the number of L1 glial cells (from wing distal tip to GSR) at different developmental stages (hours APF), as indicated in the first column. For each type of labelling, the highest and lowest numbers of labelled cells are indicated. The average number of glial cells at each stage is shown in parentheses.

analysed by time-lapse do reach adulthood and display no abnormal phenotype. Finally, wings subjected to glial and neuronal labelling after the time-lapse do not reveal major differences when compared with unprocessed wings (data not shown). Thus, this *in vivo* approach is non-invasive, highly sensitive and allows us to faithfully follow glial differentiation.

Time-lapses clearly show the simultaneous occurrence of migration and proliferation, which is more evident along the L3 nerve because of the limited number of glia (Fig. 2C, and see Movie 1 in supplementary material). Proliferation also takes place at the time of migration on L1, as documented by double labelling with anti-Repo and the anti-PH3 mitotic marker (Table 1). L1 and L3 glial cells migrate proximally and meet glia differentiating in the radius vein (Fig. 1B,C; Fig. 2C, and Movie 1). While glial precursors move as a chain on the L1 nerve from the very beginning, the three GPIs on the L3 nerve are isolated from one another (Fig. 2C). When each lineage has produced two to four cells, L3 glia become connected (Fig. 2C).

Isolated GPIs on L3 display numerous thin actin-containing processes that grow and retract in minutes (Fig. 2B, and Movie 2 in supplementary material). Such processes can be assimilated to filopodia (Gustafson and Wolpert, 1961), which are well known for their role in cell motility.

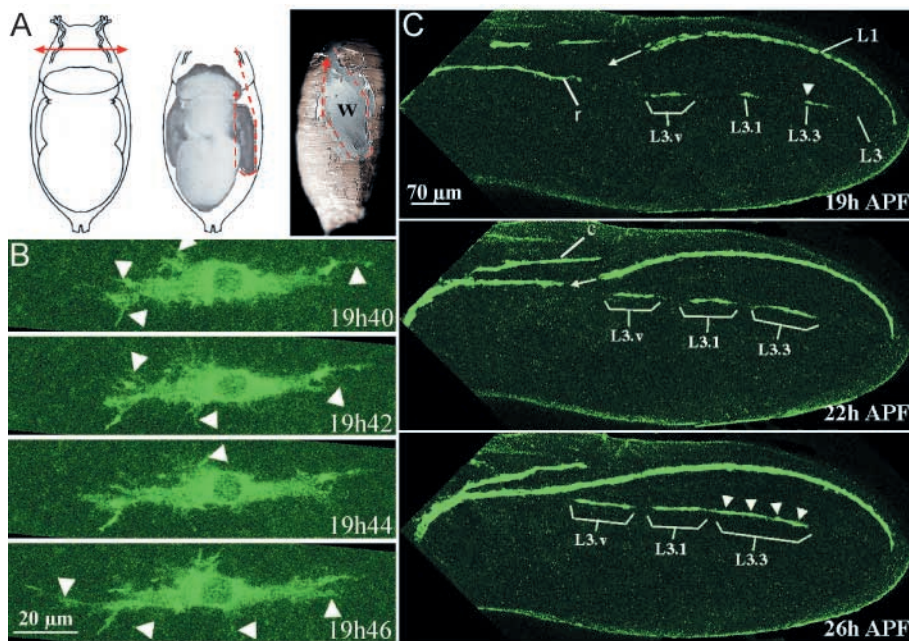


Fig. 2. Glial development followed by time-lapse. (A) Pupa preparation for time-lapse. Red lines indicate the path of puparium case dissection. The operculum is opened (left panel, straight line), and the puparium case over the wing is removed (mid and right panel, dashed lines). Left and mid panels are dorsal views; right panel is a lateral view. Anterior is to the top. W, wing. (B) *repo-actinGFP*: time-lapse images of a GPI showing dynamic cell shape and filopodia reorganisation (arrowheads). (C) Time-lapse images showing *repo-ncGFP* (nuclear and cytoplasmic GFP) labelling (see Movie 1 in supplementary material). Symbols as in Fig. 1B. Brackets indicate the glial cells originating from L3 gliogenic sensory organs. Arrows show the L1 front of migration. Arrowheads indicate the positions of L3.3 glial nuclei. Scale bars: 20 µm (B); 70 µm (C).

On L1, high glial density makes it more difficult to follow individual behaviours. Nevertheless, time-lapse analyses identify the proximal front as a landmark of directional migration (Fig. 2C, and Movie 1 in supplementary material). Cells at the front of migration or pioneer cells display very long and dynamic filopodia (Fig. 3A,D, and see Movie 3 in supplementary material) that have disappeared by the time the pioneers reach more proximal glia (data not shown). Although

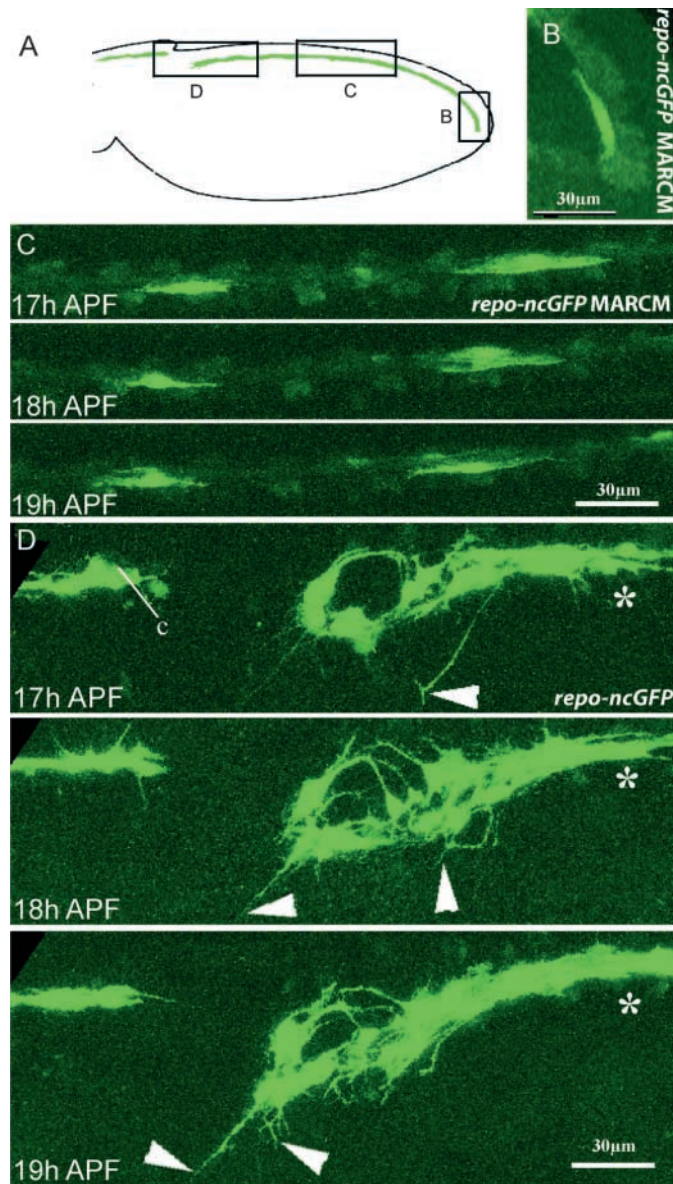


Fig. 3. Pioneer and follower L1 glial cells. (A) Schematic representation of a wing. Boxes show regions of interest on L1 (B-D) that have been analysed in different *repo-ncGFP* animals. (B,C) Individually labelled (*repo-ncGFP* MARCM clones) follower cells. (B) Distal glial cell at 17 hours APF. (C) Time-lapse sequence (17-19 hours APF) on two glial cells. (D) Time-lapse sequence (17-19 hours APF) on the whole glial population at the front of migration (see also Movie 3 in supplementary material). Pioneer glial cells display more numerous and elaborate filopodia (arrowheads) when compared with follower cells, which are more distal (see asterisk). Scale bars: 30 µm (B-D).

the precise number and position of the pioneer cells is not yet known, their presence suggests that specialised glia populate different regions of the nerve. To label individual L1 glial cells, we performed a mosaic analysis with a repressible cell marker (MARCM) (Lee and Luo, 2001) (Fig. 3B,C), using the *repo-GFP* line. By mitotic recombination, GFP expression is induced in patches of glial cells and, occasionally, isolated labelled cells are generated. This approach allowed us to formally demonstrate for the first time that, in addition to the pioneer, dynamic, glia, another migratory population showing less filopodial activity is located at more distal positions. All distal glia (25 wings analysed) show a less elaborate morphology than the pioneer cells (Fig. 3B-D), suggesting that they represent the majority of the L1 glia.

In summary, time-lapse and clonal analyses disclose the dynamic behaviour of the glial cytoskeleton, and identify pioneer and follower glia.

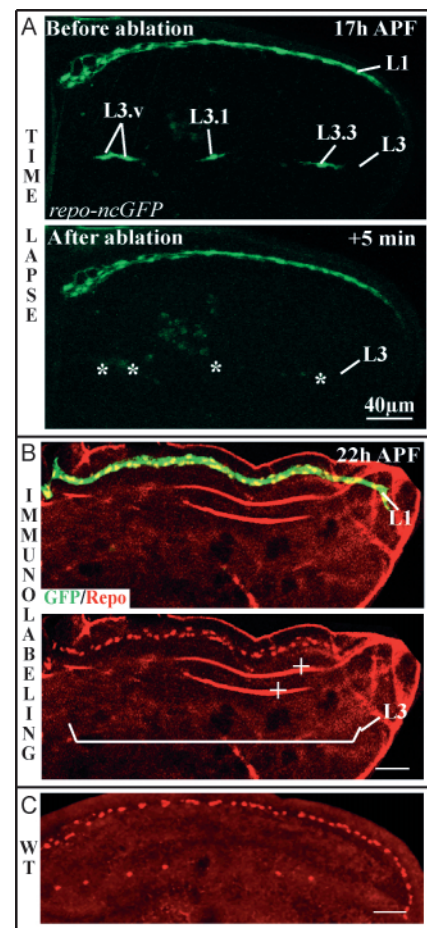


Fig. 4. Confocal-assisted cell ablation. (A) Ablation of all L3 glial lineages (L3.3, L3.1 and L3.v) at 17 hours APF on a *repo-ncGFP* wing. GFP labelling before (upper panel) and just after (lower panel) UV laser irradiation. Asterisks indicate the position of the ablated cells. (B) Immunolabelling on the same wing five hours after ablation. Notice the absence of specific Repo (upper and lower panels) and GFP (upper panel) labelling on L3 (bracket). (C) A wild-type wing at a comparable stage, labelled with anti-Repo. + indicates unspecific labelling corresponding to the wing cuticle. Scale bars: 40 µm.

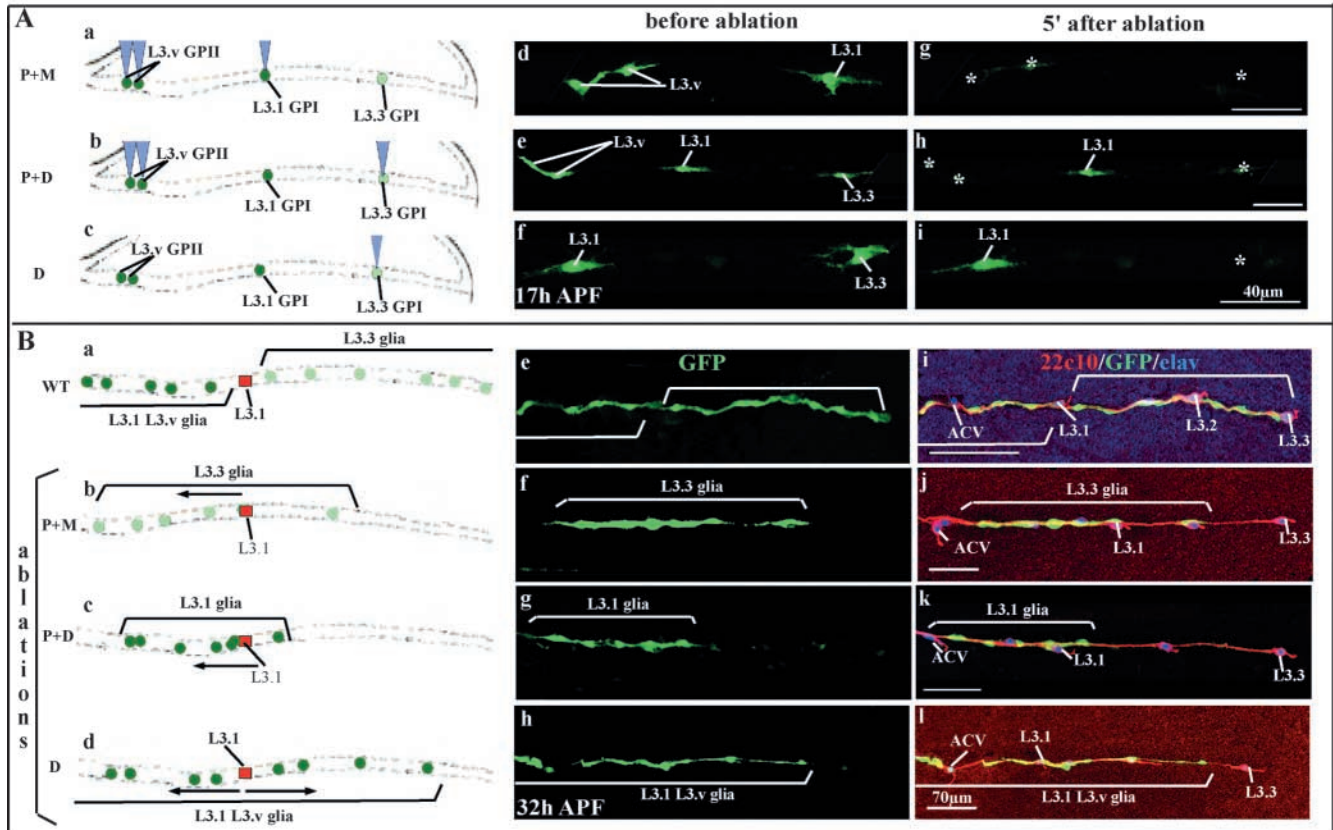


Fig. 5. Glia-glia contact inhibit migration. In all schematic drawings (A, panels a-c; B, panels a-d), distal glia are shown in light green and proximal/medial glia in dark green. Glial cells are represented by circles, neurones by red squares, the laser beam is indicated in purple. (A) Glia ablations on 17 hours APF *repo-ncGFP* wings. (a-c) Ablation of proximal/medial (L3.1 and L3.v; P+M), bilateral (L3.3 and L3.v; P+D) and distal (L3.3; D) glial cells, respectively. (d-i) GFP labelling before (d-f) and just after (g-i) ablation. Asterisks indicate the positions of the ablated cells. (B) Same wings as in A, 15 hours after cell ablation. (a-d) Schematic representations of the results. (e-l) Immunolabelling with anti-GFP (green), anti-22c10 (red; neuronal somata and axons) and anti-Elav (blue; neuronal nuclei). Symbols are as above. (e-h) anti-GFP. (i-l) Multiple labelling. Scale bars: in A, panels d-i, 40 μm; in B, panels e-l, 70 μm.

Glia-glia interactions inhibit the extent of migration

Movies on L3 glia show that cells belonging to one lineage move until they reach more proximal glial cells. Although both groups of cells continue to migrate upon establishment of contact, they tend not to intermingle, as distally located glia do not bypass proximal glia (see Movie 4 in supplementary material and Fig. 8). Moreover, glial precursor divisions give rise to cells that always move apart one from the other shortly after being produced (Movie 1). To test for the role of glia-glia interactions in cell migration, we devised a confocal-assisted ablation protocol using the *repo-GFP* line. We targeted the UV laser to a confined region of a GFP-positive nucleus, using the Leica bleachpoint function (see Materials and methods), and verified that cell death is induced in several ways. First, fading of GFP labelling in the targeted cell is induced within five minutes following UV irradiation (Fig. 4A). This was observed in all the cells that were subjected to irradiation ($n=38$). Labelling never resumed, even after hours. Second, cell irradiation results in a lack of Repo labelling. Fig. 4B shows an example of cell ablation of all L3 glia, verified by lack of both GFP and Repo labelling throughout the L3 vein. Third, bleaching glial cells using the 488 nm ray at very high intensity does not lead to death.

Indeed, bleached cells resume expressing GFP and go on dividing (data not shown).

In wild-type 33-hour APF animals, L3.3 glia populate the nerve region distal to the L3.1 neurone (Fig. 5B, panels a,e,i). Upon proximal (L3.v) and medial (L3.1) GPI killing (Fig. 5A, panels a,d,g), distal (L3.3) glia migrate more proximally than in normal wings (Fig. 5B, panels b,f,j). Thus, contacts between glial cells control migration by limiting their movement.

Glial cells have been shown to migrate in one direction, from distal to proximal (Giangrande, 1994) (Figs 1, 2). In light of the cell ablation data, we investigated whether, in addition to the extent, glia-glia contacts also control the direction of migration. We ablated distal and proximal GPIs, thereby leaving medial glia (L3.1) free to migrate in both directions over unoccupied substrate (Fig. 5A, panels b,e,h). In such bilateral ablations, L3.1 glia preferentially migrate in the proximal direction (Fig. 5B, panels b,f,i), indicating that glia-glia interactions play a minor role in directionality. This was confirmed by specifically killing the distal (L3.3) GP (Fig. 5A, panels c,f,i). In these conditions, in which L3.1 glia find unlimited space distally but not proximally, those glia occupy more distal positions than in wild-type wings or wings subjected to bilateral ablation (Fig. 5B, panels d,h,l). As

expected from glia-glia interactions playing a limited role in directional migration, the extent of over-migration observed upon ablation is much less conspicuous in a distal direction than in the proximal direction. When free to move (proximal and medial ablation), L3.3 glia migrate proximally and reach the L3.1 neurone in most cases (6/8), and, in two cases, go even further and reach the ACV (Fig. 5B panels b,f,j). By contrast, only in one case do proximal/medial glia reach the L3.3 neurone (1/7 wings) upon distal ablation (Fig. 5B, panels d,h,l). In all experiments, lack of GFP labelling in the target cells was monitored both just after and several hours after ablation (Figs 4, 5).

Altogether, these data indicate that glia can move in both directions, although they are less apt to migrate distally than proximally, and that glia-glia interactions inhibit the extent of movement.

Neurone-glia interactions control directional migration but not glial motility

In order to determine the role of neurone-glia interactions, we analysed migration in wings that lack axons. When the Notch (N^{ts1}) receptor is absent throughout wing sensory organ development, all cells within the lineage are transformed into glia. These glia, which initially form a cluster (Fig. 6A) (Van De Bor and Giangrande, 2001), eventually organise themselves in a continuous chain, indicating that they are able to migrate despite the absence of neurones (Fig. 6D,E). Interestingly, glial

cells reach more distal positions than in wild-type wings (Fig. 6E,F), suggesting that, although the axonal substrate does not control glial motility, it affects the direction of glial migration.

Hw wings display ectopic sensory organs that produce neurones and glia (Balcells et al., 1988; Blair et al., 1992; Giangrande, 1995). These neurones often send out axons that navigate distally. Although the misrouted axons are lined by glial cells, the analysis of fixed preparations could not assess the glial migratory pathways. Time-lapse analysis on *Hw* wings (Fig. 7A,B, and Movie 5 in supplementary material) enables us to show that the direction of supernumerary glia migration does correlate with that taken by underlying axons regardless of their direction. Fig. 7A shows time-lapse images from a mutant wing carrying ectopic glia on the posterior margin. While the distal glial cell migrates proximally, the proximal one divides and migrates distally. After time-lapse, the wing was labelled to check for the presence of underlying axons (Fig. 7B,C). Three glial cells are associated with two ectopic axons. The orientation taken by glial cells is in agreement with the differentiation of a proximal neurone sending an axon distally and a distal neurone sending an axon proximally. The *Hw* data strongly suggest that directional migration specifically relies on neuronal polarity rather than general polarity cues.

Altogether, time-lapse and genetic data indicate that neurone-glia interactions affect directional migration but not motility.

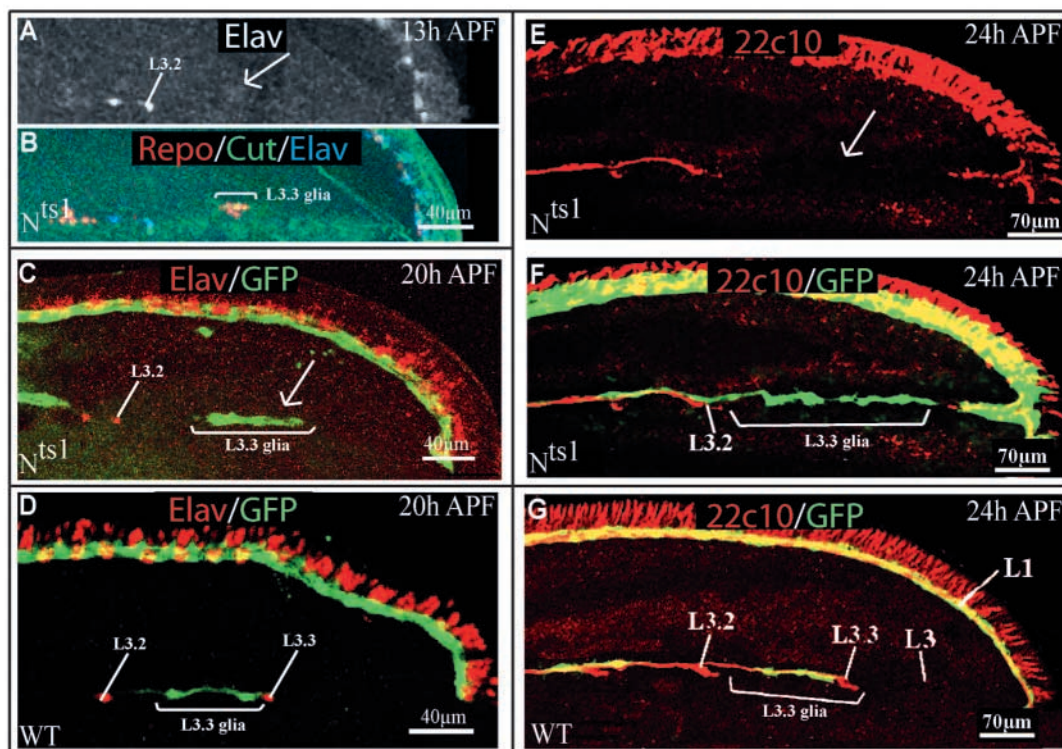


Fig. 6. Glia migration in the absence of neurones. (A-C,E,F) $N^{ts1}; N^{ts1}; repo-ncGFP$ wings after complete transformation of the L3.3 gliogenic lineage into glia immunolabelled at 13 hours (A,B), 20 hours (C) and 24 hours (F) APF. (B) Triple labelling with anti-Repo (red), anti-Elav (blue) and anti-Cut (all SOP progeny, green). (C,D) Wings labelled with anti-Elav (red) and anti-GFP (green). (E-G) Wings immunolabelled with anti-22c10 (red) and anti-GFP (green). A corresponds to the blue channel of B, and E corresponds to the red channel of F. Notice the absence of the L3.3 neurone (arrows) in the N^{ts1} wings, as shown by lack of neuronal labelling (anti-Elav in A-C; anti-22c10 in E,F). (D,G) Wild-type (WT): ($repo-ncGFP$) wings at 20 hours (D) and 24 hours (G) APF. In all panels, brackets indicate L3.3 glia. Symbols are as above. Scale bars: 40 μm (A-D); 70 μm (E-G).

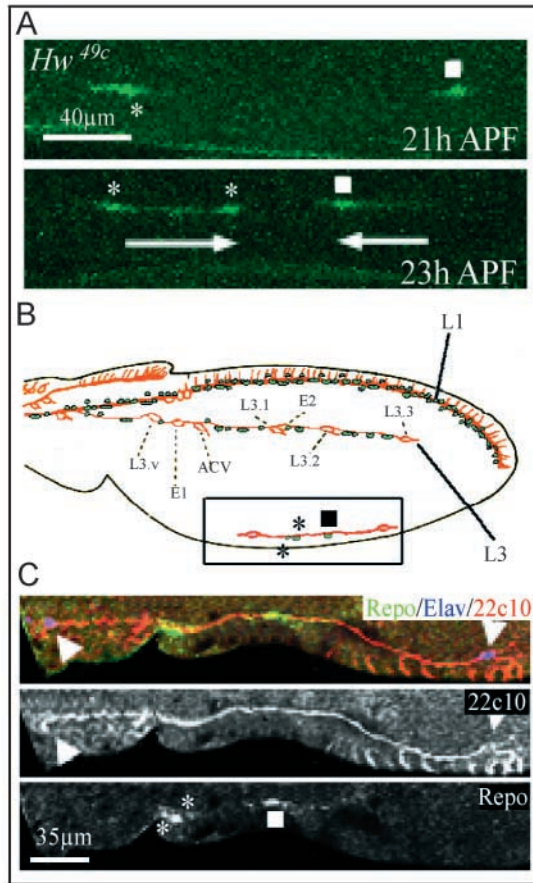


Fig. 7. Neurone-glia interactions affect directional migration. (A) Time-lapse analysis in an *Hw^{49c}; repo-ncGFP* wing posterior margin. Ectopic glia are indicated in the upper panel by an asterisk (proximal cell) and a square (distal cell). Lower panel: a proximal cell has divided, arrows show the direction of migration. (B) Schematic drawing of the same wing after immunolabelling. The posterior margin region analysed by time-lapse (A) and immunolabelling (C) is shown in the box and contains neurones (red) and glial cells (green). (C) Anti-Repo, anti-22c10 and anti-Elav labelling performed after time-lapse. Arrowheads show neuronal cell bodies. Scale bars: 40 μm (A); 35 μm (C).

Control of glial cell number

In the nervous system, the control of cell number is achieved through cell division and/or death (Hidalgo, 2002; Raff et al., 1993; Sepp and Auld, 2003). For example, glial precursors in the rat optic nerve divide extensively during development, some progeny subsequently undergoing apoptosis (Barres et al., 1992). By using several approaches, we investigated how the number of wing glia is controlled. First, we followed an individual glial lineage from 23 hours APF for almost ten hours, a time frame that includes all divisions (see Movie 6 in supplementary material). A short interval (thirteen minutes) and the use of a nuclear GFP enabled us to score for any proliferative and/or apoptotic event. At the beginning of the movie, the GPI has already divided once, and within an hour the two GPIs divide again. This example of a glial lineage of four cells shows no sign of cell death throughout the time-lapse. Seven L3.3 lineages were analysed in this way and in no

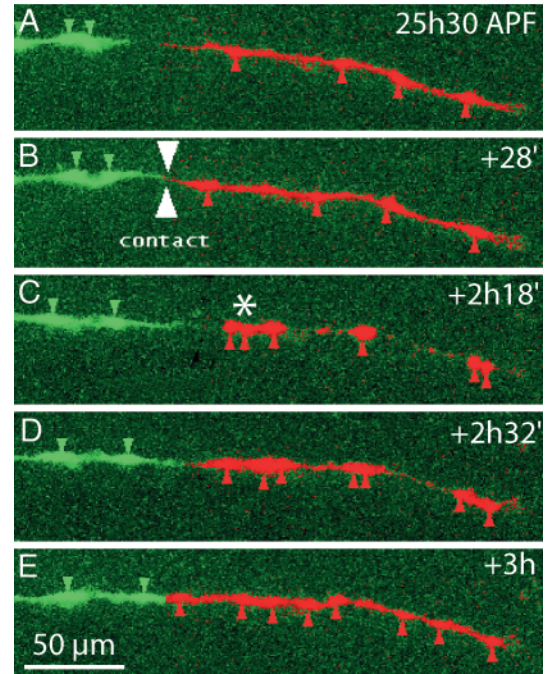


Fig. 8. Establishment of glial cell contact does not inhibit proliferation. Time-lapse images from a *repo-ncGFP* wing showing L3.3 (artificially coloured in red) and L3.1 (green) glial lineages. Nuclei are indicated by small, coloured arrowheads. (A) L3.3 and L3.1 GPIs are not in contact at 25 hours and 30 minutes APF. (B) L3.3 and L3.1 GPIs contact each other (white arrowheads) 28 minutes later. (C-E) All L3.3 GPIs divide and produce eight cells; notice that cell division entails a transient loss of contact between L3.3 and L3.1 glia (asterisk in C). Scale bar: 50 μm .

instance did we retrieve dying cells, not even in lineages containing more than four cells (data not shown). Similar results were obtained in the L3.1 lineage ($n=7$ wings analysed by time-lapse; data not shown).

As a second approach, we analysed the apoptotic profile of wing glia at six developmental stages (see Fig. S1 in supplementary material). Owing to the transient nature of the TUNEL labelling, more than six wings were analysed at each stage ($n=7$ at 17 hours, $n=40$ at 20 hours, $n=8$ at 22 hours, $n=25$ at 26 hours, $n=6$ at 30 hours and $n=10$ at 36 hours APF). Although TUNEL did label sparse cells throughout the wing, in no cases were L1 and L3 glial cells positive for TUNEL labelling. Thus, in the fly wing, the control of cell number is primarily achieved through cell division.

As glia-glia interactions control migration, we investigated whether they also affect proliferation. Homeostatic control of proliferation, a regulatory process that involves compensatory divisions, does take place in the neural crest upon cell ablation (Couly et al., 1996; McKee and Ferguson, 1984). This process, however, does not seem to occur in wing glia, as cells from different lineages keep proliferating even when they are in touch with each other ($n=13$) as shown in Fig. 8. Indeed, the four L3.3 GPIs all undergo one round of division after the L3.3 lineage establishes contact with the L3.1 glial cells. Furthermore, L1 glia keep proliferating (Table 1), even though they are in contact with each other from very early stages (Fig.

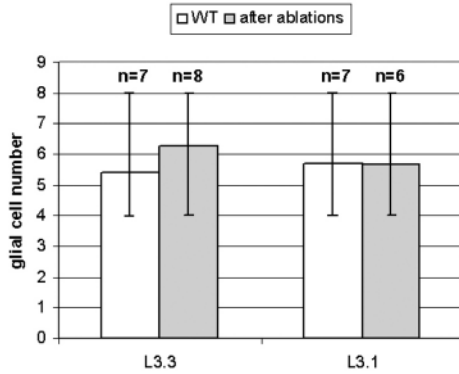


Fig. 9. Glia-glia interactions do not control proliferation. Glial cell number at 32 hours APF, after proximal/medial (L3.v and L3.1) and bilateral (L3.v and L3.3) glial cell ablation, revealing the contribution of the L3.3 and L3.1 glia, respectively. Values obtained upon ablation (grey bar) or in wild-type wings (white bar). Wild-type values were obtained by following L3.3 and L3.1 lineages in seven time-lapses. Bars indicate the highest and lowest values; *n* indicates the number of samples analysed.

2C). The formal demonstration that glia-glia contacts do not control cell division comes from the observation that, when a GPI is ablated, glial cells from the remaining lineages do not overproliferate (Figs 5, 9).

Compensatory behaviours might be lineage restricted. Indeed, although glial cells from different lineages are initially not in contact, GPI daughters always stay in touch with each other. Based on genetic (Van De Bor et al., 2000) and time-lapse data (Fig. 10C), the expected average number of cells

originating from a half lineage is three. We therefore investigated whether killing one GPI forces the other one to overproliferate (Fig. 10). L3.3 lineages were followed for several hours by time-lapse after killing either distal ($n=5$ wings) or proximal ($n=5$ wings) GPII cell. In all cases, divisions of the remaining GPI are not delayed compared with those of lineages that had not been irradiated (see Fig. 10, panel d, and Movies 7, 8 in supplementary material). Upon fixation and immunolabelling of the wing analysed *in vivo*, three cells were found, on average, for each half lineage, and in no case were more than four cells observed (Fig. 10C). Altogether, these results indicate that glial precursors have a limited proliferative potential and that glia-glia interactions do not control proliferation.

Glial cell division and polarity

Upon apico-basal division of the IIb, the GPI delaminates from the epithelium and associates with the neuronal cell body (Van De Bor et al., 2000). At the earliest stage at which GPI can be detected *in vivo*, it sends multidirectional extensions that contain microtubules (Fig. 11A, panel a). Later on, however, extensions along the proximodistal axis continue to grow, whereas the others progressively prune back so that GPI eventually grows in a polarised fashion along the underlying axon (Fig. 11A, panels b-f). This drastic reorganisation, probably reflecting the change in cell polarity that occurs upon delamination, is not observed in GPI daughters, which seem to be already proximodistally polarised at birth (data not shown). Despite such different behaviours, both GPIs and their daughters always divide along the proximodistal axis (Fig. 11B,C). The unduplicated centrosome is detectable shortly before division and is located at the front or at the rear end of

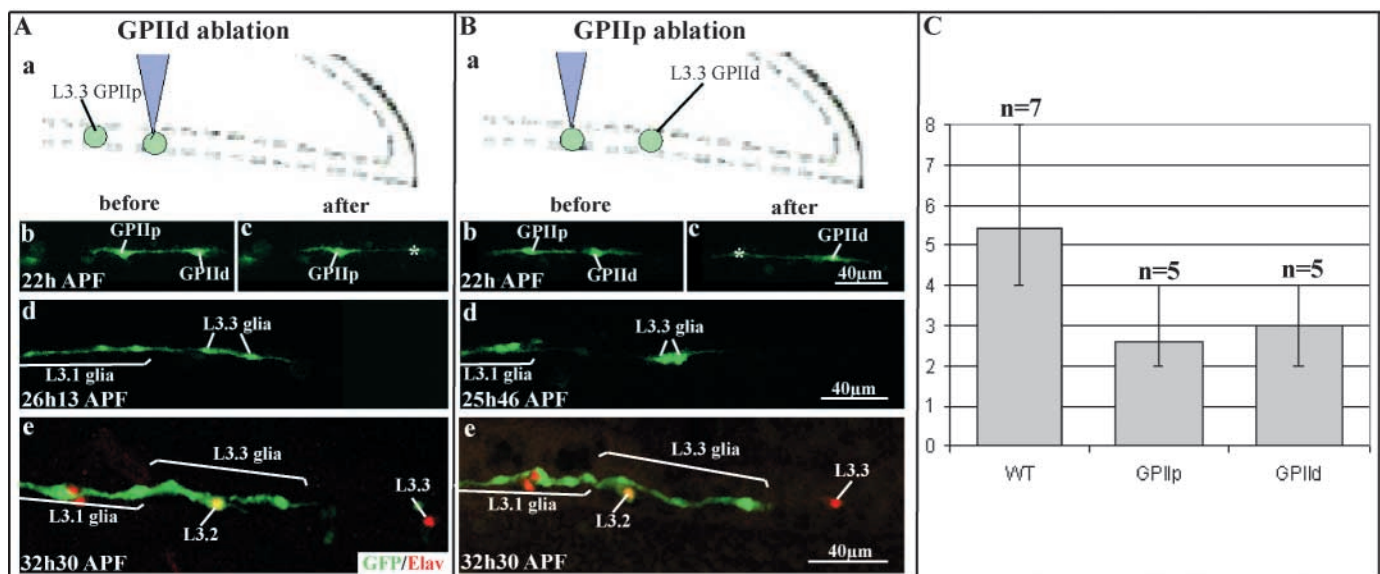


Fig. 10. Ablation within a glial lineage. (A,B) Examples of GPIIId (A) and GPIIp (B) ablations performed at 22 hours APF. Symbols are as in Fig. 5. (a) Schematic representation of the ablation. (b-d) GFP labelling before (b), just after (c) and several hours (d) after ablation. Asterisks in panel c show fading of the GFP labelling in the targeted cell. Notice (d) that the spared GPII remains labelled by GFP and undergoes division. (e) Immunolabelling at 32 hours and 30 minutes APF, using anti-GFP and anti-Elav. Brackets indicate the remaining glia progeny of L3.3 and L3.1 GPII. L3.2 indicates the L3.2 neurone. (C) Average number of glial cells at 32 hours and 30 minutes APF in a wild-type (WT) wing, and in GPIIp or GPIIId ablated wings. Glial cells from each L3.3 sublineage were followed by time-lapse; *n* indicates the number of samples analysed. Bars indicate highest and lowest values. Scale bars: 40 μ m.

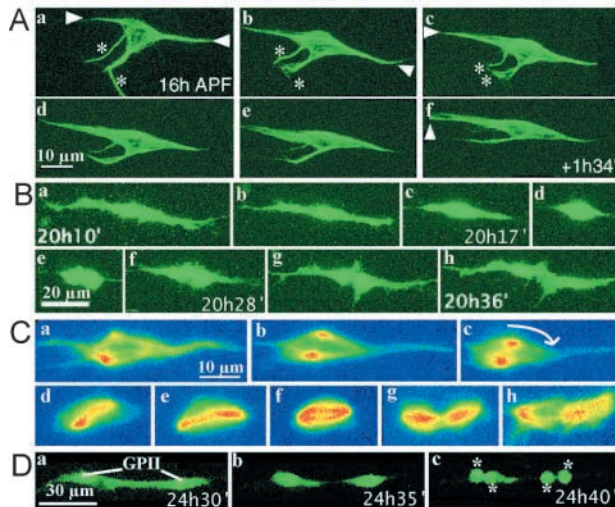


Fig. 11. Time-lapse analysis of glial cell division. (A) Time-lapse analysis of a *repo-tauGFP* GPI: (a-f) proximodistal extensions keep elongating (arrowheads), whereas the others prune back (asterisks). (B) Time-lapse sequence of a GPI division using *repo-ncGFP*. (a-d) Glial extensions rapidly prune back so that the cell adopts an almost round shape (d). Upon cell division (e), the GPIs rapidly send out novel extensions (f-h). (C) Microtubule reorganisation at division. Confocal projections, illustrating a GPI division (*repo-tauGFP*). (a-c) Colour coding allows labelling quantification and thereby the identification of centrosomes as red spots (highest GFP levels). (b,c) Centrosomes migrate and position themselves perpendicular to the orientation of division. (d-f) GFP reveals the mitotic spindle, which undergoes rotation, so that division takes place along the proximodistal axis (g,h). (D) Time-lapse sequence showing that GPIs of the same sensory organ divide synchronously. Glial nuclei are indicated by asterisks. Scale bars: 10 μm (A,C); 20 μm (B); 30 μm (D).

the cell (data not shown). Upon duplication, centrosomes move away from the pole and orient themselves perpendicular to the proximodistal axis (Fig. 11C, panels a-c). The mitotic apparatus then undergoes rotation (Fig. 11C, panels d,e) and finally orient itself along the proximodistal axis (Fig. 11C, panels f-h).

As cells of the glial lineage divide, their long extensions prune back, and cells take on an almost spherical shape (Fig. 11B). After division, daughter cells (GPIs, GPIIs and glia) elaborate novel extensions that allow axonal enwrapment.

Time-lapse data are consistent with the mode of division proposed in Fig. 1A. GPIs are of comparable size and shape, and both undergo mitosis, which is suggestive of symmetric rather than asymmetric stem-cell like divisions (Fig. 11D). Cells of the glial lineage divide rather synchronously, in contrast with previous results obtained on fixed material (Van De Bor et al., 2000). For example, GPIs of the same lineage divide within 30 minutes of one another (Fig. 11D). Cells from different lineages divide with, at the most, a one-hour time difference (see Movies 1, 4 in supplementary material). The discrepancy between fixed and living materials is probably due to the fact that anti-PH3 antibody recognises dividing cells in a transient manner (Hendzel et al., 1997).

In conclusion, glial precursors divide synchronously and symmetrically along the axis of migration.

Discussion

We present a novel genetic model, fly wing glia, to study cell migration and proliferation by time-lapse in the whole animal. We also identify individual migrating cells by clonal analysis and set up a confocal-assisted cell ablation protocol to target specific cell populations.

The combined use of cell ablation, genetic and time-lapse approaches allows us to show that: (1) glial cells undergo extensive cytoskeleton and mitotic apparatus rearrangements during movement and division; (2) pioneer glia actively explore the environment during migration; (3) neurone-glia affect directional migration but do not control glial motility; (4) glia-glia interactions control the extent of migration; and (5) the control of glial cell number is achieved via cell proliferation, which is autonomously determined.

Fly wing glia, a model system for cell movement and proliferation

The ability to move is shared by many cells in normal and pathological conditions (Gammill and Bronner-Fraser, 2003; Keller, 2002; Perego et al., 2002; Small et al., 2002; Traver and Zon, 2002). The fly wing gives us the opportunity to analyze proliferating cells moving in a chain (L1 glia) and in isolation (early L3 glia).

When we compare L1 glia with fly border and tracheal cells, both differences and similarities become apparent. First, border cells rely on an asymmetric structure, the actin based-LCE (long cellular extension), which triggers movement through a grapple and pull process (Fulga and Rorth, 2002; Geisbrecht and Montell, 2002). By contrast, wing pioneer glial cells send out numerous filopodia that dynamically assay the environment in all directions, as is also seen in tracheal cells (Ribeiro et al., 2002; Sato and Kornberg, 2002). This may reflect the fact that border cells form a cluster and move simultaneously, whereas, in the chain of glia, distal cells do not contact pioneer cells and follow the movement of adjacent, more proximal, cells. Based on time-lapse and ablation data, we propose the following model. Prior to migration, pioneer cells are free to explore the proximal axonal substrate whereas follower cells are submitted to bilateral repulsive glia-glia contacts. As pioneer cells move proximally, they free space at more distal positions. Follower cells rapidly occupy such space, thus freeing even more distal regions. This domino-type of migration proceeds until homogenous axon enwrapping is reached.

Most exploratory activity is spatially and temporally restricted as it specifically characterises cells that move on naked axons. Whether the presence of pioneer cells at the front of migration is lineage dependent or reliant on extracellular signals remains to be determined. In the future, performing ablations throughout the L1 will help to address the issue of plasticity. The presence of LCE versus pioneer filopodia may reflect different modalities of directional migration. It is known that border cells respond to chemoattractants (Fulga and Rorth, 2002; Montell, 2003), whereas glial directional migration may be driven by underlying axons (see below). Interestingly, L3 migrating and proliferating cells all show filopodia, suggesting yet a different mode of migration compared with that of cell chains (L1 glia) and clusters (border cells). Finally, glia, but not tracheal or border cells, divide as they move, suggesting that the formation of a continuous chain along the axon bundle requires both

migration and proliferation. In the future, it will be crucial to determine how the two events are coordinated.

The different features shown by border cells, trachea and glia suggest that cell specification controls motility strategies. The role of cell specification cues is further demonstrated by the fact that, even within glial cells, different lineages display distinct features. While wing GPs divide several times (Van De Bor et al., 2000) (this study), glia arising from dorsal bipolar dendritic embryonic lineages (Umesono et al., 2002) and microchaete glia (Gho et al., 1999; Reddy and Rodrigues, 1999) do not divide, the latter dying soon after birth (Fichelson and Gho, 2003). Understanding the molecular pathways specifying migratory and proliferative profiles represents one of the future challenges for developmental biologists.

Like oligodendrocyte precursors in the rat optic nerve that are controlled by an internal clock (reviewed by Durand and Raff, 2000), GPIs divide a limited number of times. Different sets of data speak in favour of an internal clock that limits the absolute number of divisions to three. First, the average number of glia derived by different sensory organs is constant (Van De Bor et al., 2000) (this study), irrespective of the number of underlying axons (L3.3 and L3.1 glia line one and four axons, respectively). Thus, the number of axons does not control proliferation. Second, time-lapse data show that divisions within and between lineages are rather synchronous. Third, mitotic clones lacking the *Glide/Gcm* (Glial cell deficient/Glial cell missing) glial promoting factor in one gliogenic sensory organ result in fewer wing glia, indicating that the remaining cells do not compensate for the missing ones (Van De Bor et al., 2000). Finally, our ablation data demonstrate a lack of compensatory divisions within and amongst glial lineages. Whether vertebrate and invertebrate clocks rely on the same signals will be a matter of future studies. In addition to the internal clock, extracellular signals may be at work and may control the fine-tuning of proliferation (four to eight cells per lineage). A role of cell-cell interactions in the control of glial proliferation has also been observed in the fly embryo (Griffiths and Hidalgo, 2004).

Specific cell-cell interactions control different aspects of migration

One of the most peculiar features of glia is that they tend to form a chain of cells. This might suggest that glial cells display affinity for axons as well as for other glial cells, the equilibrium between these affinities dictating the extent of migration and triggering the formation of a continuous glial sheath. However, even in the absence of axons (*N^{ts1}* data), glial cells form a continuous chain, rather than staying as a cluster or moving apart from one another. Thus, axons do not trigger glial cell alignment, clearly showing that glia are endowed with an intrinsic migratory potential. The chain of glia present in *N^{ts1}* wings is unbranched, as if the surrounding vein were providing a physical channel or instructive cues for migration. Although we cannot formally exclude a participation of veins in axonal navigation and/or glia migration, veinless wings still contain properly organised axons and glia (data not shown). Moreover, ectopic axons present in the intervein space of *Hw* wings carry properly lined glial cells (data not shown), thus indicating that veins are not instructive for glial migration.

One way to reconcile all data is that different types of interactions take place. On the one side, glia tend to fully

occupy and enwrap naked axons, probably in response to neuronal signals. On the other side, counteracting interactions are at work between glia. Thus, while affinity between glial cells induces them to stay together, repulsive contacts prevent them from forming a cluster and trigger the formation of a chain. The observation that the cytoplasmic processes of adjacent glia largely overlap (data not shown) is in agreement with this hypothesis, and leads us to propose that glial cells tend to reduce the extent of contact by sliding over each other. The equilibrium between all these forces allows the formation of a continuous chain and controls the extent of movement, compatibly with the substrate available for migration.

Glial cells move in a stereotyped direction and, as shown by the ablation data, do not require the presence of guide-post glia to find their way. Instead, neurone-glia interactions affect directional migration. Indeed, both in fly wings and in the zebrafish lateral line, misrouted axons result in redirected glia (Giangrande, 1995; Gilmour et al., 2002) (this study). Furthermore, in both systems, glial arrest is observed upon axonal arrest (Giangrande et al., 1993; Giangrande, 1994; Gilmour et al., 2002). The fact that glia use axons as a substrate suggests an unpredicted axonal feature. Indeed, although the polarised nature of the axon is well characterised with respect to microtubule growth, how does the axon convey directional information to the enwrapping glia?

Our data clearly show that glial migration relies on complex and dynamic glia-glia and neurone-glia interactions. Establishing time-lapse protocols that simultaneously monitor neurones and glia, or aiming at simultaneously identifying the whole glial population and a subset of glia, will be crucial to gaining a better understanding of the precise nature and role of such homo- and heterotypic interactions.

Glial cell polarity and division

Most migratory cells undergo an epithelial to mesenchymal transition that implies changes in cell polarity (Hay, 1995). Similarly, glial cells originate through the apico-basal division of the *Ib* precursor (Gho et al., 1999; Reddy and Rodrigues, 1999; Van De Bor et al., 2000). The newly formed GPIs wait almost ten hours before dividing, whereas GPIIs divide and migrate rapidly soon after birth (Van De Bor et al., 2000) (this study). By the end of this latency period, the GPI acquires a very polarised shape, and divides along the proximodistal axis. Altogether, these results indicate that a change in cell polarity occurs in the GPI, the cell that starts migrating. Thus, latency probably serves to build up the GPI competence for proliferation and migration.

The fact that glial cells divide and migrate along the same axis suggests that the signalling pathways controlling cell polarity, division and motility are coordinated. The analysis of mutations affecting these processes will be fundamental for understanding the molecular bases of their integration.

Conclusions

The development of transgenic animals carrying GFP and cell-specific promoters makes it now possible to analyse dynamic behaviours such as migration and proliferation at the level of individual cells in wild-type and mutant backgrounds. Furthermore, following the consequences of cell ablation allows analysis of the role played by cell-cell interactions. In future, combining genetics with cell biology in living animals

will give novel insights into the cellular and molecular network controlling cell movement and division in physiological and pathological conditions.

We thank P. Heitzler, J. Knoblich, A. Travers, V. Auld, H. Oda, C. Desplan, A. Brand, the Bloomington Stock Centre and the DSHB for flies and antibodies. We also thank J. L. Vonesch and D. Hentsch for help with the confocal microscopy, imaging and data processing. We thank W. B. Grueber for fruitful discussion on cell ablation. We thank all group members and P. Rorth for helpful comments on the manuscript. This work was supported by the EEC (QLG3-CT-2000-01224), INSERM, the CNRS, the Hôpital Universitaire de Strasbourg, the Human Frontier Science Program, the Ministère de la Recherche (ACI Développement) and the ARC. B.A. and V.V.d.B. were supported by MRT and ARC fellowships, respectively.

Supplementary material

Supplementary material for this article is available at <http://dev.biologists.org/cgi/content/full/131/20/5127/DC1>

References

- Ashburner, M. and Thompson, J. N. (1978). The laboratory culture of *Drosophila*. In *The Genetics and Biology of Drosophila*, Vol. 2a (ed. M. Ashburner and T. R. F. Wright), pp. 1-109. London, New York: Academic Press.
- Balcells, L., Modolell, J. and Ruiz-Gomez, M. (1988). A unitary basis for different Hairy-wing mutations of *Drosophila melanogaster*. *EMBO J.* **7**, 3899-3906.
- Barres, B. A., Hart, I. K., Coles, H. S., Burne, J. F., Voyvodic, J. T., Richardson, W. D. and Raff, M. C. (1992). Cell death and control of cell survival in the oligodendrocyte lineage. *Cell* **70**, 31-46.
- Bellaiche, Y., Gho, M., Kaltschmidt, J. A., Brand, A. H. and Schweisguth, F. (2001). Frizzled regulates localization of cell-fate determinants and mitotic spindle rotation during asymmetric cell division. *Nat. Cell Biol.* **3**, 50-57.
- Bernardoni, R., Kammerer, M., Vonesch, J. L. and Giangrande, A. (1999). Gliogenesis depends on glide/gcm through asymmetric division of neuroglioblasts. *Dev. Biol.* **216**, 265-275.
- Blair, S. S., Giangrande, A., Skeath, J. B. and Palka, J. (1992). The development of normal and ectopic sensilla in the wings of hairy and Hairy wing mutants of *Drosophila*. *Mech. Dev.* **38**, 3-16.
- Brand, A. (1995). GFP in *Drosophila*. *Trends Genet.* **11**, 324-325.
- Campbell, G., Goring, H., Lin, T., Spana, E., Andersson, S., Doe, C. Q. and Tomlinson, A. (1994). RK2, a glial-specific homeodomain protein required for embryonic nerve cord condensation and viability in *Drosophila*. *Development* **120**, 2957-2966.
- Carpenter, E. M. and Hollyday, M. (1992). The distribution of neural crest-derived Schwann cells from subsets of brachial spinal segments into the peripheral nerves innervating the chick forelimb. *Dev. Biol.* **150**, 160-170.
- Couly, G., Grapin-Botton, A., Coltey, P. and le Douarin, N. M. (1996). The regeneration of the cephalic neural crest, a problem revisited, the regenerating cells originate from the contralateral or from the anterior and posterior neural fold. *Development* **122**, 3393-3407.
- Durand, B. and Raff, M. (2000). A cell-intrinsic timer that operates during oligodendrocyte development. *Bioessays* **22**, 64-71.
- Etienne-Manneville, S. and Hall, A. (2003). Cdc42 regulates GSK-3beta and adenomatous polyposis coli to control cell polarity. *Nature* **421**, 753-756.
- Fichelson, P. and Gho, M. (2003). The glial cell undergoes apoptosis in the microchaete lineage of *Drosophila*. *Development* **130**, 123-133.
- Friedl, P. and Wolf, K. (2003). Tumour-cell invasion and migration, diversity and escape mechanisms. *Nat. Rev. Cancer* **3**, 362-374.
- Fujita, S. C., Zipursky, S. L., Benzer, S., Ferrus, A. and Shotwell, S. L. (1982). Monoclonal antibodies against the *Drosophila* nervous system. *Proc. Natl. Acad. Sci. USA* **79**, 7929-7933.
- Fulga, T. A. and Rorth, P. (2002). Invasive cell migration is initiated by guided growth of long cellular extensions. *Nat. Cell Biol.* **4**, 715-719.
- Gammill, L. S. and Bronner-Fraser, M. (2003). Neural crest specification, migrating into genomics. *Nat. Rev. Neurosci.* **4**, 795-805.
- Geisbrecht, E. R. and Montell, D. J. (2002). Myosin VI is required for E-cadherin-mediated border cell migration. *Nat. Cell Biol.* **4**, 616-620.
- Gerlich, D., Beaudouin, J., Kalbfuss, B., Daigle, N., Eils, R. and Ellenberg, J. (2003). Global chromosome positions are transmitted through mitosis in mammalian cells. *Cell* **112**, 751-764.
- Gho, M., Bellaiche, Y. and Schweisguth, F. (1999). Revisiting the *Drosophila* microchaete lineage, a novel intrinsically asymmetric cell division generates a glial cell. *Development* **126**, 3573-3584.
- Giangrande, A. (1994). Glia in the fly wing are clonally related to epithelial cells and use the nerve as a pathway for migration. *Development* **120**, 523-534.
- Giangrande, A. (1995). Proneural genes influence gliogenesis in *Drosophila*. *Development* **121**, 429-438.
- Giangrande, A., Murray, M. A. and Palka, J. (1993). Development and organization of glial cells in the peripheral nervous system of *Drosophila melanogaster*. *Development* **117**, 895-904.
- Gilmour, D. T., Maischein, H. M. and Nusslein-Volhard, C. (2002). Migration and function of a glial subtype in the vertebrate peripheral nervous system. *Neuron* **34**, 577-588.
- Griffiths, R. L. and Hidalgo, A. (2004). Prospero maintains the mitotic potential of glial precursors enabling them to respond to neurons. *EMBO J.* **23**, 2440-2450.
- Gustafson, T. and Wolpert, L. (1961). Studies on the cellular basis of morphogenesis in the sea urchin embryo, directed movements of primary mesenchyme cells in normal and vegetalized larvae. *Exp. Cell Res.* **24**, 64-79.
- Halter, D. A., Urban, J., Rickert, C., Ner, S. S., Ito, K., Travers, A. A. and Technau, G. M. (1995). The homeobox gene *repo* is required for the differentiation and maintenance of glia function in the embryonic nervous system of *Drosophila melanogaster*. *Development* **121**, 317-332.
- Hay, E. D. (1995). An overview of epithelio-mesenchymal transformation. *Acta Anat.* **154**, 8-20.
- Henzel, M. J., Wei, Y., Mancini, M. A., van Hooser, A., Ranalli, T., Brinkley, B. R., Bazett-Jones, D. P. and Allis, C. D. (1997). Mitosis-specific phosphorylation of histone H3 initiates primarily within pericentromeric heterochromatin during G2 and spreads in an ordered fashion coincident with mitotic chromosome condensation. *Chromosoma* **106**, 348-360.
- Hidalgo, A. (2002). Interactive nervous system development, control of cell survival in *Drosophila*. *Trends Neurosci.* **25**, 365-370.
- Kakita, A. (2001). Migration pathways and behavior of glial progenitors in the postnatal forebrain. *Hum. Cell* **14**, 59-75.
- Kaltschmidt, J. A., Davidson, C. M., Brown, N. H. and Brand, A. H. (2000). Rotation and asymmetry of the mitotic spindle direct asymmetric cell division in the developing central nervous system. *Nat. Cell Biol.* **2**, 7-12.
- Keil, T. A. (1997). Functional morphology of insect mechanoreceptors. *Microsc. Res. Tech.* **39**, 506-531.
- Keller, R. (2002). Shaping the vertebrate body plan by polarized embryonic cell movements. *Science* **298**, 1950-1954.
- Lauffenburger, D. A. and Horwitz, A. F. (1996). Cell migration, a physically integrated molecular process. *Cell* **84**, 359-369.
- Lee, T. and Luo, L. (2001). Mosaic analysis with a repressible cell marker (MARCM) for *Drosophila* neural development. *Trends Neurosci.* **24**, 251-254.
- McKee, G. J. and Ferguson, M. W. (1984). The effects of mesencephalic neural crest cell extirpation on the development of chicken embryos. *J. Anat.* **139**, 491-512.
- Meili, R. and Firtel, R. A. (2003). Follow the leader. *Dev. Cell* **4**, 291-293.
- Mollereau, B., Wernet, M. F., Beaufils, P., Killian, D., Pichaud, F., Kuhnlein, R. and Desplan, C. (2000). A green fluorescent protein enhancer trap screen in *Drosophila* photoreceptor cells. *Mech. Dev.* **93**, 151-160.
- Montell, D. J. (2003). Border-cell migration, the race is on. *Nat. Rev. Mol. Cell Biol.* **4**, 13-24.
- Murray, M. A., Schubiger, M. and Palka, J. (1984). Neuron differentiation and axon growth in the developing wing of *Drosophila melanogaster*. *Dev. Biol.* **104**, 259-273.
- Nadarajah, B. and Parnavelas, J. G. (2002). Modes of neuronal migration in the developing cerebral cortex. *Nat. Rev. Neurosci.* **3**, 423-432.
- Perego, C., Vanoni, C., Massari, S., Raimondi, A., Pola, S., Cattaneo, M. G., Francolini, M., Vicentini, L. M. and Pietrini, G. (2002). Invasive behaviour of glioblastoma cell lines is associated with altered organisation of the cadherin-catenin adhesion system. *J. Cell Sci.* **115**, 3331-3340.
- Raff, M. C., Barres, B. A., Burne, J. F., Coles, H. S., Ishizaki, Y. and Jacobson, M. D. (1993). Programmed cell death and the control of cell survival, lessons from the nervous system. *Science* **262**, 695-700.
- Reddy, G. V. and Rodrigues, V. (1999). A glial cell arises from an additional

- division within the mechanosensory lineage during development of the microchaete on the *Drosophila notum*. *Development* **126**, 4617-4622.
- Ribeiro, C., Ebner, A. and Affolter, M.** (2002). In vivo imaging reveals different cellular functions for FGF and Dpp signaling in tracheal branching morphogenesis. *Dev. Cell* **2**, 677-683.
- Robinow, S. and White, K.** (1991). Characterization and spatial distribution of the ELAV protein during *Drosophila melanogaster* development. *J. Neurobiol.* **22**, 443-461.
- Sato, M. and Kornberg, T. B.** (2002). FGF is an essential mitogen and chemoattractant for the air sacs of the *drosophila* tracheal system. *Dev. Cell* **3**, 195-207.
- Sepp, K. J. and Auld, V. J.** (2003). Reciprocal interactions between neurons and glia are required for *Drosophila* peripheral nervous system development. *J. Neurosci.* **23**, 8221-8230.
- Sepp, K. J., Schulte, J. and Auld, V. J.** (2000). Developmental dynamics of peripheral glia in *Drosophila melanogaster*. *Glia* **30**, 122-133.
- Sepp, K. J., Schulte, J. and Auld, V. J.** (2001). Peripheral glia direct axon guidance across the CNS/PNS transition zone. *Dev. Biol.* **238**, 47-63.
- Small, J. V., Stradal, T., Vignal, E. and Rottner, K.** (2002). The lamellipodium, where motility begins. *Trends Cell Biol.* **12**, 112-120.
- Traver, D. and Zon, L. I.** (2002). Walking the walk, migration and other common themes in blood and vascular development. *Cell* **108**, 731-734.
- Umesono, Y., Hiromi, Y. and Hotta, Y.** (2002). Context-dependent utilization of Notch activity in *Drosophila* glial determination. *Development* **129**, 2391-2399.
- Van de Bor, V. and Giangrande, A.** (2001). Notch signaling represses the glial fate in fly PNS. *Development* **128**, 1381-1390.
- Van de Bor, V. and Giangrande, A.** (2002). glide/gcm, at the crossroads between neurons and glia. *Curr. Opin. Genet. Dev.* **12**, 465-472.
- Van de Bor, V., Walther, R. and Giangrande, A.** (2000). Some fly sensory organs are gliogenic and require glide/gcm in a precursor that divides symmetrically and produces glial cells. *Development* **127**, 3735-3743.
- Verkhusha, V. V., Tsukita, S. and Oda, H.** (1999). Actin dynamics in lamellipodia of migrating border cells in the *Drosophila* ovary revealed by a GFP-actin fusion protein. *FEBS Lett.* **445**, 395-401.
- Welch, M. D., Mallavarapu, A., Rosenblatt, J. and Mitchison, T. J.** (1997). Actin dynamics in vivo. *Curr. Opin. Cell Biol.* **9**, 54-61.
- Wood, W., Jacinto, A., Grose, R., Woolner, S., Gale, J., Wilson, C. and Martin, P.** (2002). Wound healing recapitulates morphogenesis in *Drosophila* embryos. *Nat. Cell Biol.* **4**, 907-912.
- Xiong, W. C., Okano, H., Patel, N. H., Blendy, J. A. and Montell, C.** (1994). *repo* encodes a glial-specific homeo domain protein required in the *Drosophila* nervous system. *Genes Dev.* **8**, 981-994.